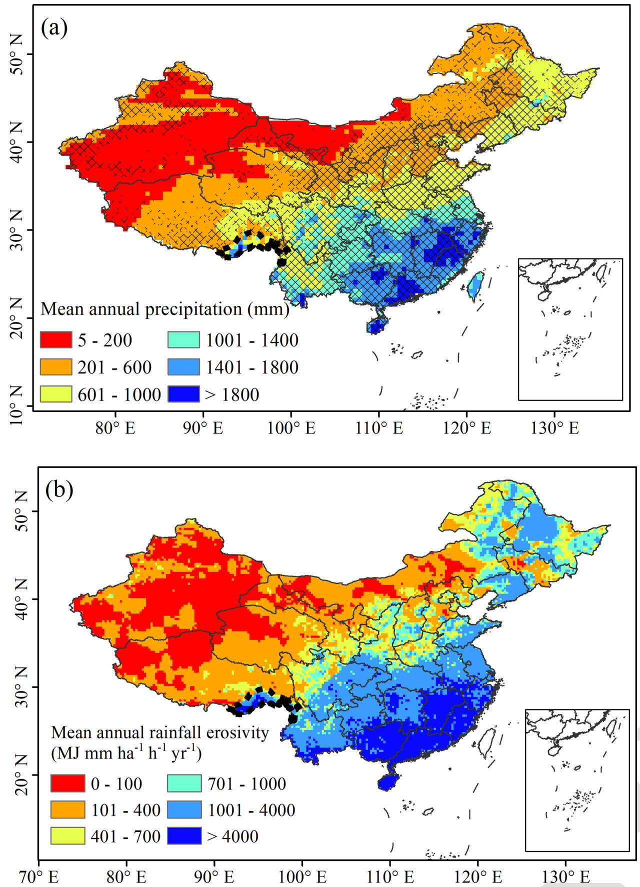

Figure 4. **(a)** Spatial distribution of mean annual precipitation in China. Grids without crossed diagonal lines indicate areas without station records. The dashed black line marks the Dawang–Chayu region. **(b)** Spatial distribution of mean annual rainfall erosivity across mainland China.

3.2 Comparison with previous studies

The newly generated mean annual rainfall erosivity map for mainland China is compared with the widely used maps from Panagos et al. (2017) and Yue et al. (2022). Compared to the map developed by Panagos et al. (2017), there is a good correlation in regions with mean annual rainfall erosivity below 10 000 MJ mm ha^{-1} h^{-1} yr^{-1}. However, in areas with annual rainfall erosivity exceeding 10 000 MJ mm ha^{-1} h^{-1} yr^{-1}, our estimates are significantly higher (Fig. 5a). When compared with the map by Yue et al. (2022), the overall correlation is good with annual rainfall erosivity less than 10 000 MJ mm ha^{-1} h^{-1} yr^{-1}. In regions with mean annual rainfall erosivity exceeding 10 000 MJ mm ha^{-1} h^{-1} yr^{-1}, the differences are larger, but no clear pattern is observed (Fig. 5b). In summary, our results correlate well with existing studies in areas with lower mean annual rainfall erosivity but show significant differences in high-erosivity areas.

A further comparison was conducted across the nine river basins in China (Fig. 6). The Hai and Huai river basins show the largest differences in mean and median mean annual rainfall erosivity values among the three datasets. Although some differences in performance are observed between basins, no consistent pattern emerges. These discrepancies primarily stem from variations in spatial and temporal resolution of the precipitation data and the algorithms used (Table 1). The algorithms in these studies are based on recommendations from RUSLE and RUSLE2. The E calculations of RUSLE are approximately 12 % lower than those from RUSLE2 for precipitation intensities below 35 mm h^{-1} but 2 % higher for intensities above 100 mm h^{-1} (Nearing et al., 2017). Regarding I_{30}, 1 h precipitation data cannot accurately capture this value. Unlike other studies, this research utilized the largest set of in situ precipitation records but over a shorter time coverage. Since the R factor typically describes the potential of precipitation to cause erosion over a long-term climate scale, ideally spanning 20 years (Renard et al., 1997), using short-term data may introduce bias. Ayat et al. (2022) reported an increasing trend of extreme subhourly rainfall near Sydney, Australia, over the last 2 decades, though no similar evidence exists for hourly or daily scales. However, trends in extreme subhourly rainfall over mainland China remain unclear. This study provides the mean annual rainfall erosivity map for the past decade, acknowledging potential biases, particularly in the context of climate change.

4 Impacts of precipitation data and algorithms on estimating rainfall erosivity

Variations in rainfall erosivity data and algorithms are the primary reasons for discrepancies in rainfall erosivity estimation. In this section, E values for erosive precipitation events are calculated using the kinetic energy methods from RUSLE and RUSLE2, evaluating how different kinetic energy algorithms affect rainfall erosivity estimation. To assess the impact of temporal resolution of precipitation data on the accuracy of I_{30}, I_{30} values for erosive rainfall events were calculated using precipitation data at different temporal resolutions (1 min vs. 1 h). A total of 300 stations across China were randomly selected, using minute-level and hour-level precipitation data from 2020–2022 for comparison.

Figure 7a and b show the mean E and I_{30} for erosive rainfal[illegible]nts across mainland China during 2020–2022. The me[illegible] event E value is 6.2 MJ ha^{-1}, ranging from 1.8 to ~~12.5~~ TS2 MJ ha^{-1}, and shows a decreasing trend from southeast to northwest. The mean event I_{30} value is 18.9 mm h^{-1}, ranging from 3.0 to 34.9 mm h^{-1}, with two notable centers in the southern and central parts of China (Beijing–Tianjin–Hebei region; Shanxi, Henan, and Shandong provinces). Next, the differences between E computation using RUSLE and RUSLE2 were analyzed. For minute-level data, the ratio of the average event kinetic energy computed using RUSLE2 to RUSLE is approximately 1.09, while it is 1.15 for hourly data (Fig. 7c and d). CE1 The analysis was further extended to

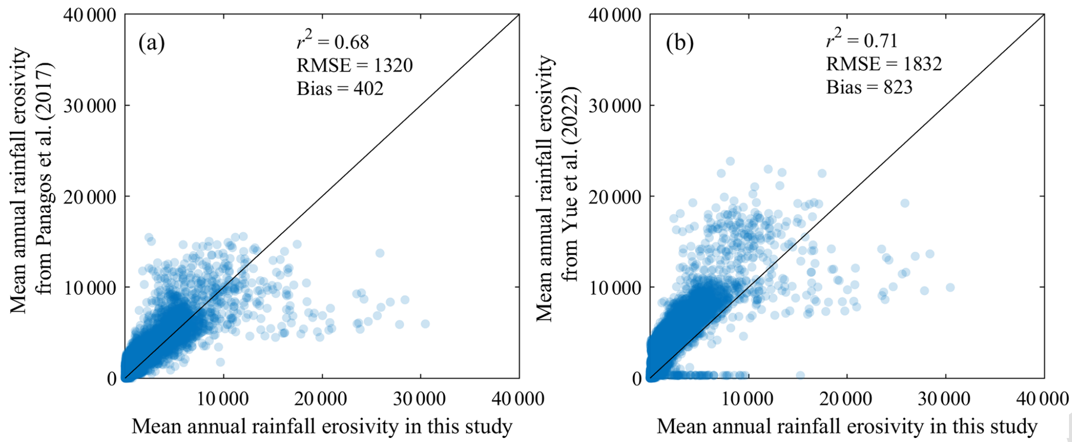

Figure 5. Comparisons between the newly developed mean annual rainfall erosivity map and existing maps (Panagos et al., 2017; Yue et al., 2022) (unit: MJ mm ha^{-1} h^{-1} yr^{-1}).

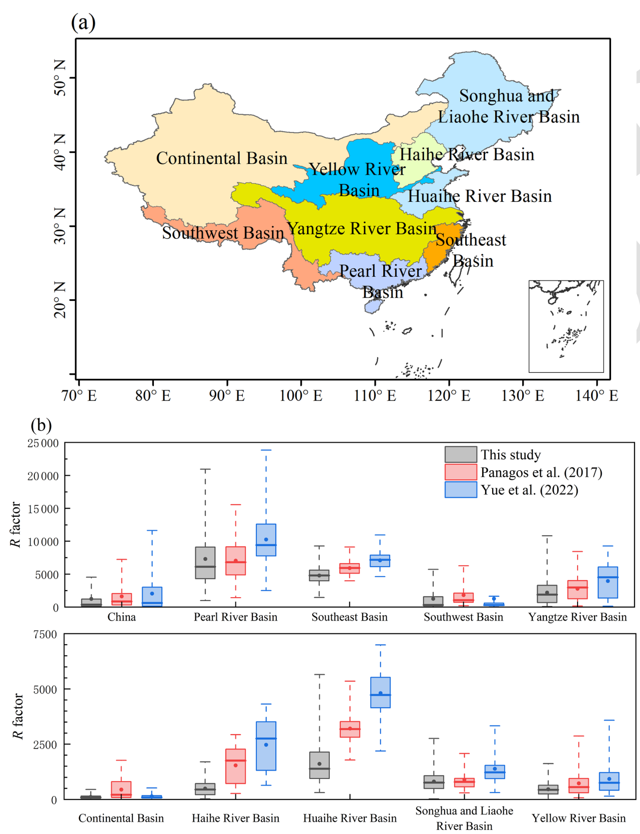

Figure 6. **(a)** The nine basins in China and **(b)** boxplots of mean annual rainfall erosivity across basins (unit: MJ mm ha^{-1} h^{-1} yr^{-1}). Grey, red, and blue boxes represent different mean annual rainfall erosivity maps from this study, Panagos et al. (2017), and Yue et al. (2022), respectively. TS1

assess the impact of temporal resolution on E and I_{30} calculations. Based on RUSLE's kinetic energy algorithm, results show that values computed from minute-level data are 1.21 times higher than those from hourly data, with more significant differences in the northwest (Fig. 7e). The impact on I_{30} is even more pronounced, with minute-level data yielding values 1.72 times higher than those from hourly data (Fig. 7f). This analysis highlights that I_{30} values exceed E at a national scale and are more sensitive to both temporal resolution of precipitation data and algorithm selection. Accurate computation of I_{30} is therefore essential for reliable rainfall erosivity estimation, underscoring the importance of high-temporal-resolution data in achieving precise rainfall erosivity estimates.

5 Data availability

The dataset is available from the National Tibetan Plateau/Third Pole Environment Data Center (https://doi.org/10.11888/Terre.tpdc.301206; Chen, 2024).

6 Conclusions

The rainfall erosivity of individual rainfall events is determined by two parameters: the E and I_{30}. High-spatiotemporal-resolution ground precipitation data provide the most accurate calculations for both E and I_{30}, resulting in the most reliable rainfall erosivity estimates. Accordingly, this study used nearly 10 years of 1 min in situ precipitation data from 60 129 stations to estimate the mean annual rainfall erosivity across mainland China. The main findings are as follows:

1. The mean annual rainfall erosivity across mainland China shows significant spatial variability, with a regional average of approximately 1241 MJ mm ha^{-1} h^{-1} yr^{-1}.

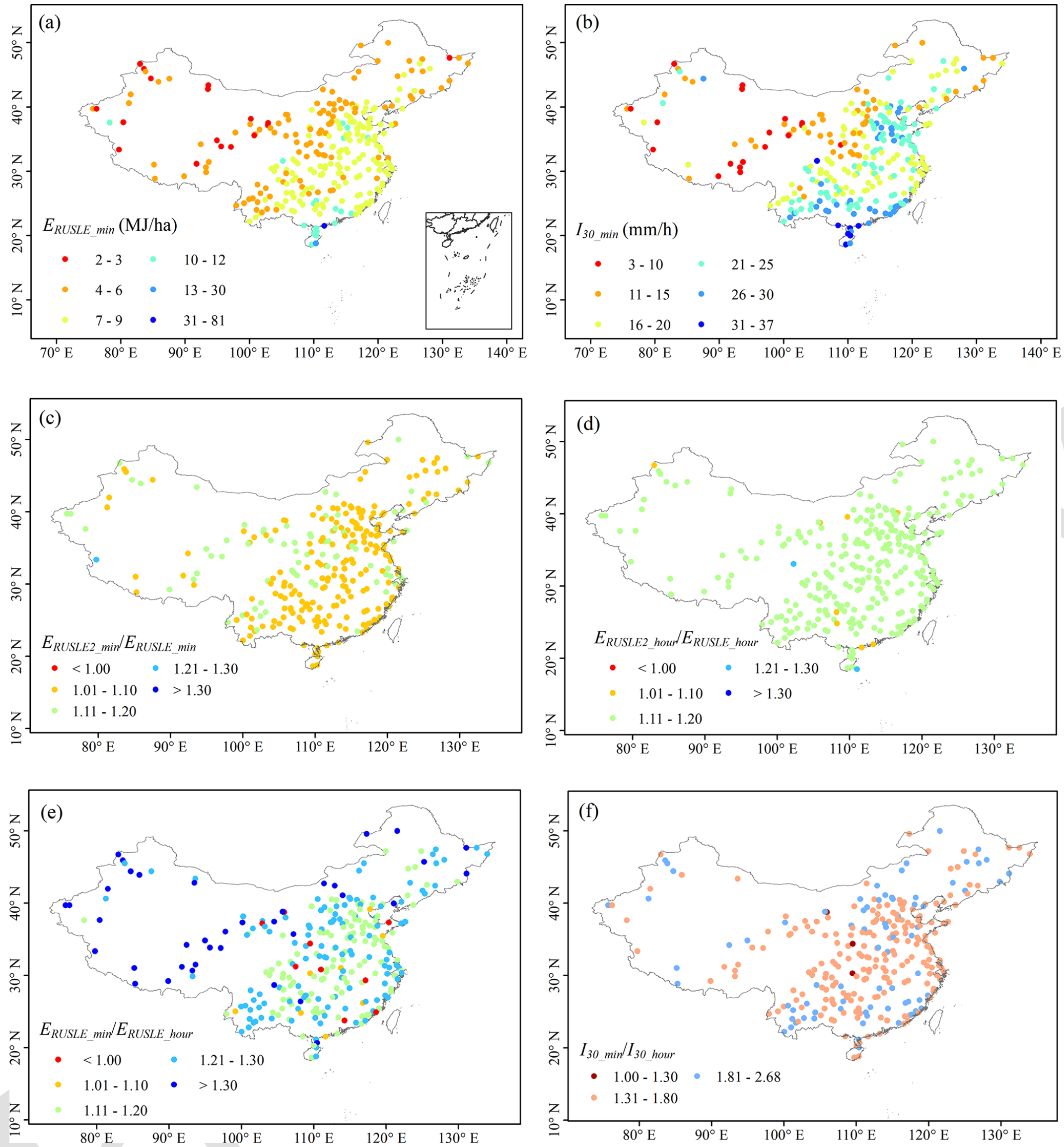

Figure 7. Spatial distribution of **(a)** mean kinetic energy (E) and **(b)** maximum 30 min rainfall intensity (I_{30}) of erosive rainfall events during 2020–2022. **(c)** Ratio of E calculated using RUSLE and RUSLE2 methods based on 1 min precipitation data. **(d)** Same as **(c)** but for 1 h data. **(e)** Ratio of E calculated using the RUSLE method for 1 min vs. 1 h data. **(f)** I_{30} calculated using 1 min vs. 1 h data. The subscript "min" indicates results based on 1 min data, while "hour" refers to 1 h data. Subscripts "RUSLE" and "RUSLE2" indicate the methods used to estimate E.

2. Compared to previous studies, this newly released dataset presents lower mean annual rainfall erosivity values across mainland China by 31 %–65 %, with significant differences across various river basins.

3. With current technology, the accuracy of determining I_{30} during erosive rainfall events is much lower than that of E. The main source of deviation in rainfall erosivity estimation is the uncertainty in I_{30}.

This newly developed dataset, based on high-resolution ground precipitation observations from the recent decade, can enhance the accuracy of soil erosion forecasting when combined with other factors in RUSLE or RUSLE2, such as newly released K factor maps (Gupta et al., 2024) and cover-management factors. Furthermore, rainfall erosivity can be viewed as a characteristic of rainfall events, offering spatial insights into precipitation-induced disasters in China.

Supplement. The supplement related to this article is available online at [the link will be implemented upon publication].